Electronic Supplementary Information

Low-power STMAS – breaking through the limit of large quadrupolar interactions in high-resolution solid-state NMR spectroscopy

Ivan Hung* and Zhehong Gan

National High Magnetic Field Laboratory, 1800 East Paul Dirac Drive, Tallahassee, FL 32310, USA
E-mail address: hung@magnet.fsu.edu

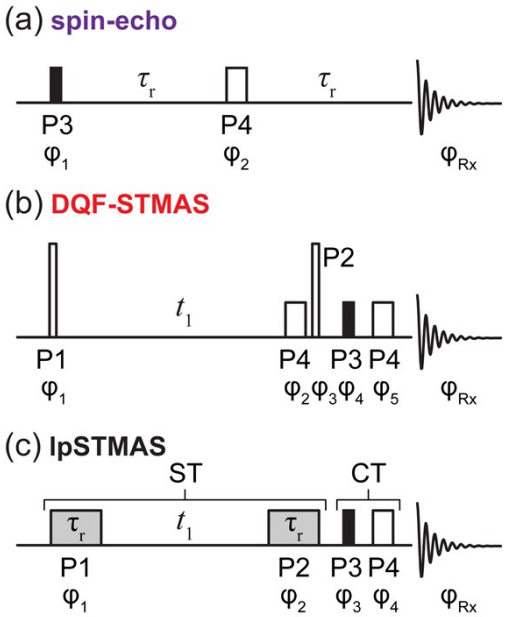

Fig. S1. Pulse sequences used for the (a) spin-echo, (b) DQF-STMAS, and (c) lpSTMAS experiments. All pulses are applied on-resonance with the CTs, except the P1 and P2 pulses for lpSTMAS which are applied at an offset far from the CT while still in the ST ssb manifold. Phase cycles: (a) $\varphi_1 = 0$, $\varphi_2 = 0123$, $\varphi_{Rx} = 0202$; (b) $\varphi_1 = \{0\}*4$ $\{2\}*4$, $\varphi_2 = \{0\}*8$ $\{2\}*8$, $\varphi_3 = 0123$, $\varphi_4 = 0$, $\varphi_5 = \{0\}*16$ $\{1\}*16$ $\{2\}*16$ $\{3\}*16$, $\varphi_{Rx} = 0202\ 2020\ 2020\ 0202\ 2020\ 0202\ 0202\ 2020$; (c) $\varphi_1 = 02$, $\varphi_2 = 0$, $\varphi_3 = 0011\ 2233$, $\varphi_4 = \{0\}*8$ $\{1\}*8$ $\{2\}*8\{3\}*8$, $\varphi_{Rx} = 0231\ 2013\ 2013\ 0231$, where the phase values correspond to multiples of 90°. Hypercomplex acquisition was performed using States-TPPI by changing (b) φ_3 by -45° and (c) φ_2 by -90°.

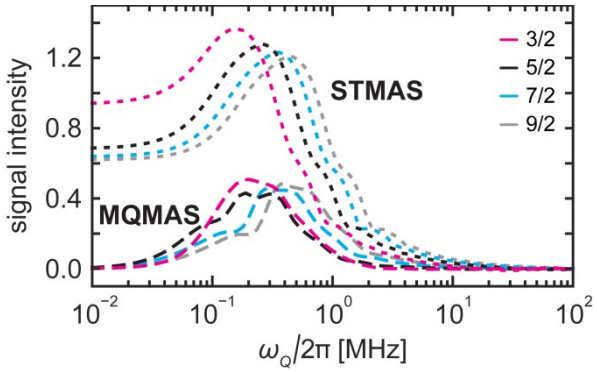

Fig. S2. Simulations of the maximum signal for the MQMAS, STMAS and lpSTMAS experiments as a function of $\omega_Q = 2\pi \cdot \nu_Q = 3C_Q/[2S(2S + 1)]$ for different spin-quantum numbers $S = 3/2$ (magenta), 5/2 (black), 7/2 (cyan), and 9/2 (gray). A three-pulse z-filter sequence (P1 - t_1 - P2 - ZF - P3 - acq) was used for all simulations with $t_1 = (1/\nu_r)$ - (P1/2) - (P2/2), where the $|+3/2\rangle \leftrightarrow |-3/2\rangle$ triple-quantum (3Q) transition was selected during t_1 for MQMAS, and the innermost $|\pm3/2\rangle \leftrightarrow |\pm1/2\rangle$ satellite-transitions (STs) were selected during t_1 for STMAS. The signal intensity is normalized to the simulated signal of a CT-selective one-pulse direct-excitation spectrum. Simulations were performed using SIMPSON[1] with an asymmetry parameter $\eta_Q = 0$, a MAS frequency of $\nu_r = 16$ kHz, the zcw986 set of crystallite angles, and only the effects of first-order quadrupolar coupling. The pulse sequence parameters for MQMAS were P1 = 6.7 μs, P2 = 1.5 μs, and a *rf* field of $\nu_1 = 100$ kHz; and for STMAS P1 = 2.5 μs, P2 = 2.5 μs, and $\nu_1 = 100$ kHz. A pulse P3 = $0.25/[\nu_1(S + 1/2)]$ was used in all instances with $\nu_1 = 10$ kHz.

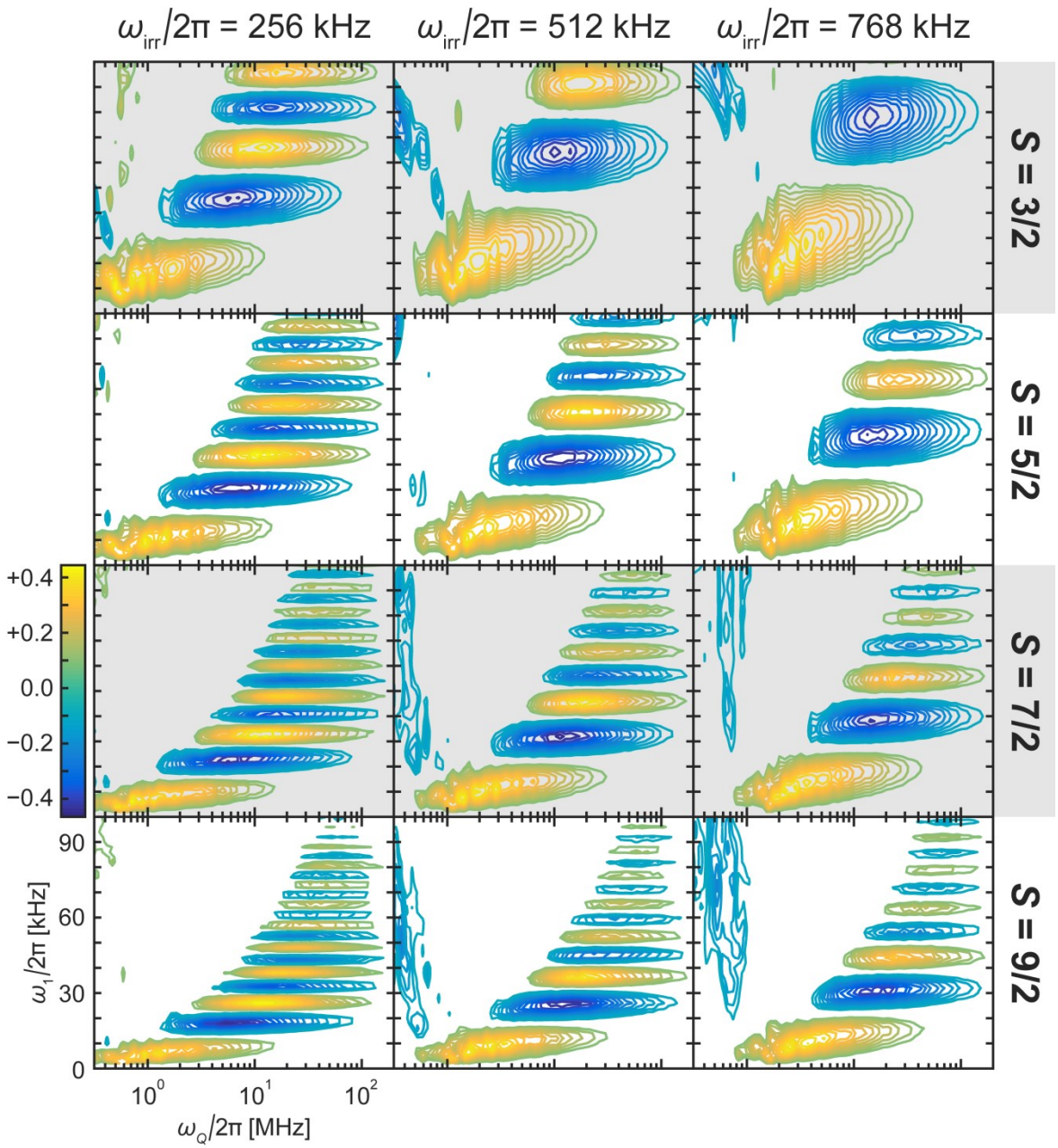

Fig. S3. Simulated lpSTMAS signal intensity for S = 3/2, 5/2, 7/2, and 9/2 at $\omega_r/2\pi$ = 16 kHz as a function of ω_1 and ω_Q, normalized to CT-selective one-pulse direct-excitation spectra. The innermost |±3/2> ↔ |±1/2> satellite-transitions were selected during t_1 in all instances. The P1 and P2 pulses were applied at offsets $\omega_{irr}/2\pi$ of +256, +512, and +768 kHz, while P3 was applied on-resonance with the central-transition. The oscillations between positive and negative intensity along the vertical dimension represent nutation of the ST magnetization around the *rf* field ω_1 at the fixed P1 = P2 = 62.5 μs.

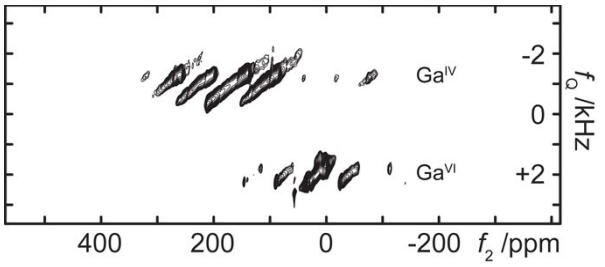

Fig. S4. Experimental 2D ^{71}Ga lpSTMAS spectrum of β-Ga_2O_3 after Q-shearing. The base contour level is set at 2% of the maximum intensity.

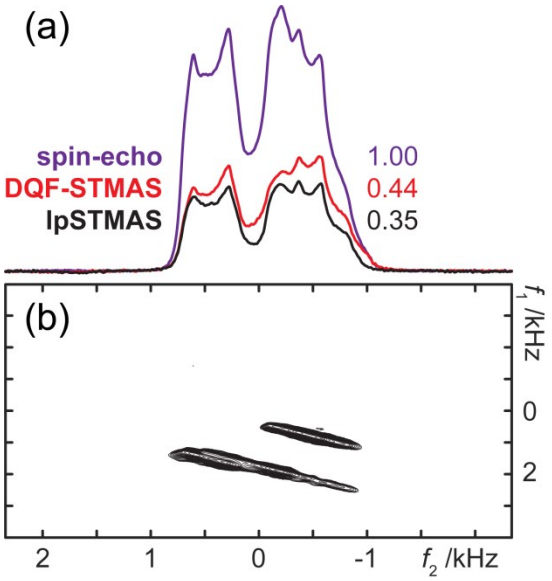

Fig. S5. (a) Experimental comparison of the ^{87}Rb DQF-STMAS and lpSTMAS signal intensity of $RbNO_3$ with a spin-echo. Spectra were recorded at B_0 = 14.1 T, ν_r = 16 kHz with a recycle delay of 0.5 s and 32 averaged transients. The spin-echo spectrum was acquired with P3 = 20 μs and P4 = 40 μs at ν_1 = 6.25 kHz. The DQF-STMAS spectrum was acquired with $t_1 = (1/\nu_r)$ - (P1/2) - (P2/2) - P4, P1 = P2 = 1.9 μs at $\nu_1 \sim 80$ kHz, and P3 = 20 μs and P4 = 40 μs at ν_1 = 6.25 kHz. The lpSTMAS spectrum was acquired with $t_1 = (1/\nu_r)$ - (P1/2) - (P2/2) = 0, P1 = P2 = $(1/\nu_r)$ = 62.5 μs at ν_1 = 12 kHz, and P3 = 20 μs at ν_1 = 6.25 kHz. All pulses were applied on-resonance with the central-transitions, except the P1 and P2 pulses for lpSTMAS which were applied at an offset of ν_{irr} = +384 kHz, as optimized empirically for maximum overall signal. (b) 2D ^{87}Rb lpSTMAS spectrum of $RbNO_3$ showing a negligible CT-CT autocorrelation ridge. The base contour level is set at 5% of the maximum intensity.

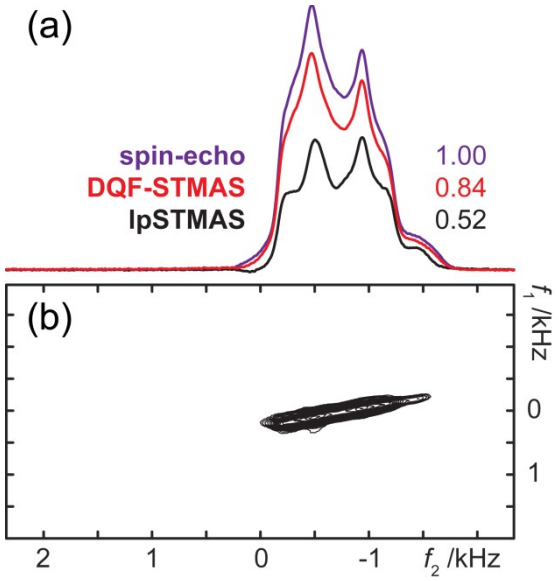

Fig. S6. (a) Experimental comparison of the ^{27}Al DQF-STMAS and lpSTMAS signal intensity of $AlPO_4$-berlinite with a spin-echo. Spectra were recorded at B_0 = 14.1 T, ν_r = 16 kHz with a recycle delay of 30 s and 16 averaged transients. The spin-echo spectrum was acquired with P3 = 20 μs and P4 = 40 μs at ν_1 = 4.2 kHz. The DQF-STMAS spectrum was acquired with $t_1 = (1/\nu_r)$ - (P1/2) - (P2/2) - P4, P1 = 1.0 μs and P2 = 1.25 μs at ν_1 = 71 kHz, and P3 = 20 μs and P4 = 40 μs at ν_1 = 4.2 kHz. The lpSTMAS spectrum was acquired with $t_1 = (1/\nu_r)$ - (P1/2) - (P2/2) = 0, P1 = P2 = $(1/\nu_r)$ = 62.5 μs at ν_1 = 5.5 kHz, and P3 = 20 μs at ν_1 = 4.2 kHz. All pulses were applied on-resonance with the central-transition, except the P1 and P2 pulses for lpSTMAS which were applied at an offset of ν_{irr} = +192 kHz, as optimized empirically for maximum overall signal. (b) 2D ^{27}Al lpSTMAS spectrum of $AlPO_4$-berlinite showing a negligible CT-CT autocorrelation ridge. The base contour level is set at 5% of the maximum intensity.